Clinical Science (2024) **138** 1287–1304
https://doi.org/10.1042/CS20241144

PORTLAND PRESS

Research Article

IFN-γ induces acute graft-versus-host disease by promoting HMGB1-mediated nuclear-to-cytoplasm translocation and autophagic degradation of p53

Shiyu Wang[1,2,3,4], Tingting Cheng[1,2,3,4], Xu Chen[1,2,3,4], Cong Zeng[1,2,3,4], Wei Qin[1,2,3,4] and Yajing Xu[1,2,3,4]

[1]Department of Hematology, Xiangya Hospital, Central South University, Changsha, China; [2]National Clinical Research Center for Hematologic Diseases, the First Affiliated Hospital of Soochow University, Soochow, China; [3]National Clinical Research Center for Geriatric Diseases (Xiangya Hospital), Changsha, China; [4]Hunan Hematologic Neoplasms Clinical Medical Research Center, Changsha, China

Correspondence: Yajing Xu (xyyajingxu@csu.edu.cn)

Acute graft-versus-host disease (aGVHD) poses a significant impediment to achieving a more favourable therapeutic outcome in allogeneic hematopoietic stem cell transplantation (allo-HSCT). Our prior investigations disclosed a correlation between p53 down-regulation in CD4+ T cells and the occurrence of aGVHD. Notably, the insufficiency of the CCCTC-binding factor (CTCF) emerged as a pivotal factor in repressing p53 expression. However, the existence of additional mechanisms contributing to the reduction in p53 expression remains unclear. Interferon (IFN)-γ, a pivotal proinflammatory cytokine, assumes a crucial role in regulating alloreactive T-cell responses and plays a complex part in aGVHD development. IFN-γ has the capacity to induce autophagy, a vital catabolic process facilitating protein degradation, in various cell types. Presently, whether IFN-γ participates in the development of aGVHD by instigating the autophagic degradation of p53 in CD4+ T cells remains an unresolved question. In the present study, we demonstrated that heightened levels of IFN-γ in the plasma during aGVHD promoted the activation, proliferation, and autophagic activity of CD4+ T cells. Furthermore, IFN-γ induced the nuclear-to-cytoplasm translocation and autophagy-dependent degradation of p53 in CD4+ T cells. The translocation and autophagic degradation of p53 were contingent upon HMGB1, which underwent up-regulation and translocation from the nucleus to the cytoplasm following IFN-γ stimulation. In conclusion, our data unveil a novel mechanism underlying p53 deficiency in CD4+ T cells among aGVHD patients. This deficiency is induced by IFN-γ and relies on autophagy, establishing a link between IFN-γ, HMGB1-mediated translocation, and the autophagic degradation of p53.

Introduction

Acute graft-versus-host disease (aGVHD) is a prevalent immune complication that arises subsequent to allogeneic hematopoietic stem cell transplantation (allo-HSCT), and is linked to elevated morbidity and mortality [1]. The pathophysiology of aGVHD manifests in three distinct phases: initiation phase, T-cell activation, and the effector phase. During the T-cell activation phase, host antigen-presenting cells (APCs) activate alloreactive donor CD4+ and CD8+ T cells, which assume a pivotal role in the development of aGVHD [2]. Therefore, elucidating the specific mechanism for T cells overactivation is crucial for understanding the pathogenesis of aGVHD and figuring out a feasible way to prevent it.

The pivotal tumour suppressor p53, primarily locating in the nuclear, orchestrates tumour suppression through apoptosis induction, cell cycle arrest and DNA repair. Recent murine studies have linked p53 deficiency to autoimmune and inflammatory diseases [3–5]. Our prior work revealed that p53 was significantly down-regulated in CD4+ T cells from patients with aGVHD compared with the non-aGVHD

Received: 15 June 2024
Revised: 03 September 2024
Accepted: 23 September 2024

Accepted Manuscript online: 23 September 2024
Version of Record published: 11 October 2024

Clinical Science (2024) **138** 1287–1304
https://doi.org/10.1042/CS20241144

group. CD4+ T cells exhibiting insufficient p53 expression undergo over-activation and proliferation under stimulation by substantial amounts of IL-2, leading to inflammatory damage in diverse organs among aGVHD patients. Additionally, we identified that the inadequacy of the CCCTC-binding factor (CTCF), a multifunctional transcription factor, represents a critical factor in repressing p53 expression [6]. Nevertheless, the existence of other mechanisms contributing to the reduction in p53 expression remains unclear.

Autophagy, an essential catabolic process facilitating the delivery of cytoplasmic material, including organelles and proteins, to lysosomes for degradation [7,8]. Autophagy supports T-cell activation, proliferation, differentiation, function, and ultimately, memory T-cell maintenance [9]. Several studies have demonstrated autophagy activated T cells [10], and an increase in autophagy in CD4+ T cells upon activation [9,11]. Moreover, unlike autophagosomes of unstimulated cells, those upon CD4+ T cell activation lack organelles and instead induce protein degradation [11]. The above findings suggest a close relationship between autophagy and T cells activation. However, whether the autophagic activity increased in CD4+ T cells from aGVHD patients, thereby leading to p53 autophagic degradation remains unknown.

Interferon (IFN)-γ, the sole type II IFN, functions as a pivotal regulator of alloreactive T-cell responses that mediate GVHD [12]. Inhibition of JAK1/2, the downstream signaling molecules of IFN-γ, significantly impedes the polarization and proliferation of activated T cells, down-regulates activation markers, and diminishes proinflammatory cytokine production [13]. Notably, emerging evidence suggests that IFN-γ augments autophagy in various cell types, including macrophages [14], mouse CD4+ T lymphocytes [15], cervical cancer cells [16], and microglial cells [17]. These findings prompt an exploration into whether IFN-γ promotes activation and autophagic activity in CD4+ T cells, inducing nuclear export and autophagic degradation of p53, thereby facilitating the cells over-activation and proliferation under IL-2 stimulation and mediating aGVHD development.

High mobility group box 1 (HMGB1), a highly conserved nuclear protein stabilizing chromatin structure and modulating gene transcription [18], predominantly resides in the nucleus [19]. During cell activation, HMGB1 can translocate to the cytoplasm and extracellular space [20]. Our previous findings unveiled a significant increase in HMGB1 expression in aGVHD CD4+ T cells, with its expression correlating with the severity of aGVHD [21]. Other studies have demonstrated that IFN-γ up-regulates HMGB1 expression in mouse mesangial cells and mediates its nuclear-to-cytoplasm translocation in macrophages [22,23]. In addition, HMGB1 binds p53 within the nucleus and cytosol [24]. Nevertheless, the role of IFN-γ in the expression and subcellular localization of HMGB1 in CD4+ T cells during aGVHD remains undefined; whether HMGB1 participates in p53 nuclear export and autophagic degradation remains unclear.

In the present study, we demonstrated that IFN-γ promotes autophagic activity in CD4+ T cells and induces nuclear-to-cytoplasm shift and autophagic degradation of p53 in the cytoplasm of CD4+ T cells. Moreover, we identified that IFN-γ not only up-regulates HMGB1 expression but also modulates its nuclear export and cytoplasmic accumulation. Additionally, HMGB1 was proven to be the crucial regulator for nuclear-to-cytoplasm transport and autophagic degradation of p53. In summary, our study identifies an autophagy-dependent degradation of p53 in CD4+ T cells from aGVHD patients induced by IFN-γ.

Materials and methods

Patients

A total of 27 patients who underwent allo-HSCT between 2022 and 2023 at the Central of Hematopoietic Stem Cell Transplantation of Xiangya Hospital were included in the present study. The research adhered to international ethical guidelines for biomedical research involving human subjects. Approval for the study protocol was obtained from the Human Ethics Committee of Xiangya School of Medicine, Central South University. All participants provided signed informed consent in accordance with the Declaration of Helsinki. Table 1 presents the clinical characteristics of the patients. The assessment of aGVHD was based on clinical symptoms following established criteria [25]. Patients were categorized into two groups based on the presence or absence of aGVHD. Peripheral blood samples were collected from patients diagnosed with aGVHD before initiating therapy (n=13). For the control group (n=14), according to the onset time of aGVHD patients, samples were collected from patients who did not develop aGVHD after allo-HSCT at the same time point. Additionally, normal CD4+ T cells were obtained from health professionals recruited from Xiangya Hospital.

Isolation, culture, and transfection of CD4+ T cells

CD4+ T cells were isolated from 40 ml venous peripheral blood using human CD4 beads (17952, Stemcell) as per the manufacturer's instructions. The cells were cultured in RPMI 1640 (Basalmedia Technologies, China) supplemented

Table 1 Patient and graft characteristics

Characteristics	Non-aGVHD	aGVHD
Number of patients	14	13
Median age (range), years	32 (7–50)	35 (17–54)
Gender, *n* (%)		
Male	11 (78.6)	9 (69.2)
Female	3 (21.4)	4 (30.8)
Diagnosis, *n* (%)		
AML/MDS	6 (42.8)	4 (30.8)
ALL	4 (28.6)	9 (69.2)
Others	4 (28.6)	0
Donor-patient sex matched, *n* (%)		
Matched	9 (64.3)	6 (46.2)
Mismatched	5 (35.7)	7 (53.8)
Donor-patient blood type matched, *n* (%)		
Matched	10 (71.4)	8 (61.5)
Mismatched	4 (28.6)	5 (38.5)
No. of HLA mismatched, *n* (%)		
1	2 (14.3)	0
2-3	4 (28.6)	1 (7.7)
4-5	8 (57.1)	8 (61.5)
Donor, *n* (%)		
MSD	0	2 (15.4)
HID	12 (85.7)	9 (69.2)
URD	2 (14.3)	2 (15.4)
Cytogenetic, *n* (%)		
Normal	6 (42.9)	5 (38.5)
Abnormal	5 (35.7)	7 (53.8)
Unknown	3 (21.4)	1 (7.7)
Disease status before HSCT, *n* (%)		
CR1	9 (64.3)	9 (69.2)
PR/NR	1 (7.1)	2 (15.4)
Others	4 (28.6)	2 (15.4)
WBC count at diagnosis, *n* (%)		
≥50,000 per mm^3	4 (28.6)	5 (38.5)
<50,000 per mm^3	6 (42.8)	6 (46.1)
Unknown	4 (28.6)	2 (15.4)
Pretransplant MRD+, *n* (%)	1 (7.1)	2 (15.4)
Infused MNCs, $\times 10^8$ /kg (range)	12.97 (8.5–21.36)	12.84 (8–22.68)
Infused CD34+ cells, $\times 10^6$ /kg (range)	5.34 (2.55–6.85)	5.68 (1.78–10.8)
Grades I-II acute GVHD, *n* (%)		10 (76.9)
Grades III-IV acute GVHD, *n* (%)		3 (23.1)

Abbreviations: ALL, acute lymphoblastic leukemia; AML, acute myeloid leukemia; HID, haploidentical donor; HLA, human leukocyte antigen; MDS, myelodysplastic syndrome; MNC, mononuclear cell; MRD, minimal residual diseases; MSD, matched sibling donor; URD unrelated donors; WBC, white blood count.

with 10% fetal bovine serum (FBS) and 1% penicillin/streptomycin. Gene interference and overexpression plasmids were transfected into 2×10^6 CD4+ T cells using the Human T cell Nucleofector Kit and Amaxa Nucleofector (Lonza). Briefly, CD4+ T cells were isolated, resuspended in 100 µl human T cell Nucleofector solution, and mixed with the plasmids. The resulting mixture was electrotransfected with Nucleofector program V-024 on an Amaxa Nucleofector. Transfected cells were cultured in RPMI 1640 containing 10% FBS at 37°C with 5% CO_2 and collected 48 h later.

Plasmids

HMGB1 shRNA plasmid has exhibited excellent interference effect in other study [26]. Accordingly, the selected HMGB1 and TP53 shRNA sequences were synthesized and inserted into pGPU6/GFP/Neo plasmid

Clinical Science (2024) **138** 1287–1304
https://doi.org/10.1042/CS20241144

Table 2 Primer sequences for real-time qPCR

	Forward primer	Reverse primer
P53	CCTCAGCATCTTATCCGAGTGG	TGGATGGTGGTACAGTCAGAGC
HMGB1	GCGAAGAAACTGGGAGAGATGTG	GCATCAGGCTTTCCTTTAGCTCG
GAPDH	GTCTCCTCTGACTTCAACAGCG	ACCACCCTGTTGCTGTAGCCAA

vectors by GenePharma (Shanghai, China). The wild-type TP53 and mutant TP53 L348,350A were generated by GenePharma (Shanghai, China) and subcloned into the pEX-6 (pGCMV/MCS/RFP/Neo) overexpression plasmid vectors (GenePharma, Shanghai, China). The target sequences were as follows: HMGB1-shRNA: 5′-CCGGGATGCAGCTTATACGAAATAACTCGAGTTATTTCGTATAAGCTGCATCTTTTTG-3′; TP53 shRNA: 5′-GACTCCAGTGGTAATCTAC-3′.

Proliferation of CD4+ T cells

CD4+ T cells were cultured in 12-well plates (1×10^6/ml), stimulated with recombinant human IL-2 (100 IU/ml, 200-02, Peprotech) in RPMI 1640. In the IFN-γ stimulation group, IFN-γ (50 ng/ml, 300-02, Peprotech) was added simultaneously with IL-2. After 24, 48, 72, and 96 h, the stimulated CD4+ T cells were seeded into 96-well plates. Subsequently, 10 μl of Cell Counting Kit-8 (CCK-8) reagent (NCM Biotech, China) was added to each well and incubated at 37°C with 5% CO_2 for 2 h in the incubator. Absorbance was measured at 450 nm on a microplate reader.

RNA isolation and real-time PCR

Total RNA was extracted from CD4+ T cells using Trizol Reagent (Invitrogen). The SweScript All-in-One First-Strand cDNA Synthesis SuperMix for qPCR (G3337-50, Servicebio, China) was employed for reverse transcription into cDNA following the manufacturer's instructions. Real-time PCR was performed in triplicate on a QuantStudio 7 Flex (Thermo Fisher Scientific) using the 2× Universal Blue SYBR Green qPCR Master Mix (G3326-15, Servicebio, China), following the manufacturer's instructions. Relative mRNA levels were normalised to glyceraldehyde-3-phosphate dehydrogenase (GAPDH) mRNA using the $2^{-\Delta\Delta CT}$ method. The primer sequences are listed in Table 2.

Western blotting

CD4+ T cells were lysed with RIPA Lysis Buffer (NCM Biotech, China) mainly containing 50mM Tris (pH 7.6), 150 mM NaCl, 1% NP-40, 0.5% sodiumdeoxycholate and 0.1% SDS, as well as proteinase inhibitor cocktail (NCM Biotech, China) and phosphatase inhibitor cocktail III (TargetMol, China). Lysates were clarified at 12,000 × ***g*** and 4°C for 15 min, and protein concentration was determined using the BCA protein assay kit (KeyGEN Biotech, China). Proteins were separated by 10% sodium dodecyl sulfate-polyacrylamide gel electrophoresis (SDS-PAGE) and transferred onto PVDF membranes (Millipore). The membranes were then blocked with 5% skim milk in Tris-buffered saline containing Tween-20 (TBST) for 2 h at room temperature, washed twice with TBST, and incubated overnight at 4°C with primary antibodies, including rabbit anti-p53 (1:1000, 10442-1-AP, Proteintech), mouse anti-p53 (1:1000, 2524, Cell Signaling Technology), rabbit anti-HMGB1 (1:6000, ab79823, Abcam), rabbit anti-phospho-STAT1 Ser727 (1:2500, ab109461, Abcam), mouse anti-Lamin B1(1:5000, 66095-1-Ig, Proteintech), rabbit anti-LC3I/II (1:1000, 14600-1-AP, Proteintech), mouse anti-LC3I/II (1:1000, 83506S, Cell Signaling Technology), rabbit anti-p62/SQSTM1 (1:5000, 18420-1-AP, Proteintech), and rabbit anti-GAPDH (1:20000, 10494-1-AP, Proteintech) antibodies. The membranes were washed with TBST and incubated with HRP-conjugated secondary antibodies, including goat anti-mouse (1:10,000, SA00001-1, Proteintech) and goat anti-rabbit (1:10000, SA00001-2, Proteintech) antibodies for 1 h at room temperature. Detection was performed with enhanced chemiluminescence (ECL) (NCM Biotech, China).

Co-immunoprecipitation

Cellular proteins were extracted with Western and IP Lysis Buffer (Byotime, China) mainly containing 20 mM Tris (pH 7.5), 150 mM NaCl, 1% Triton X-100, sodium pyrophosphate, β-glycerophosphate, EDTA, Na_3VO_4 and leupeptin, as well as proteinase inhibitor cocktail (NCM Biotech, China). Subsequently, 2 μg of anti-p53 antibodies (10442-1-AP, Proteintech) were incubated with Protein A/G Magnetic Beads (MedChemExpress) on a rotor at room temperature for 30 min. Then, antibody-magnetic beads complexes were added to protein lysates and incubated overnight at 4°C with shaking. The following day, the precipitated complexes were washed three times with chilled

Western and IP Lysis Buffer (Byotime, China). The proteins were eluted using 1× SDS-PAGE Loading Buffer (NCM Biotech, China) and then analyzed by Western blotting with anti-p53 and anti-HMGB1 antibodies.

Flow cytometric analysis

The expression of CD69 antigen was detected by flow cytometry 24 h after IFN-γ stimulation, while the expression of CD40L antigens was detected 48 h post-stimulation. CD4+ T-cell suspensions (1×10^5 cells) were incubated with PE-conjugated anti-human CD69 (310905, Biolegend) and CD40L (310805, Biolegend) antibodies for 15 min at room temperature, washed with 2 ml phosphate-buffered saline (PBS) containing 1% FBS (PBS/FBS), and centrifuged at 400 × ***g*** for 5 min. Supernatants were discarded, and cells were resuspended in 0.5 ml PBS/FBS. In the apoptosis assay, cells were collected and stained with the Annexin V-FITC/PI apoptosis kit (Byotime, China). Data were acquired with a FACSCanto II flow cytometer (Becton Dickinson) and analyzed using Flowjo software (Becton Dickinson).

Enzyme-linked immunosorbent assay (ELISA)

IFN-γ in the plasma was analyzed by an ELISA kit (EK180-96, Multisciences Biotech, China). The procedure was performed as indicated by the manufacturer. Briefly, a polystyrene microplate of 96-well pre-coated with a monoclonal antibody specific for IFN-γ was used for each test. After final staining and washing, the optical density was determined.

Immunocytochemistry

Cells were harvested, washed with PBS, and fixed with 4% paraformaldehyde (Byotime, China) for 15 min at room temperature. Subsequently, permeabilization was carried out using 0.1% Triton X-100 (Solarbio, China) in PBS for 10 min. Blocking was performed with 3% bovine serum albumin (BSA) in PBS for 1 h, followed by overnight incubation at 4°C with primary antibodies. After PBS washing, the cells were incubated with Alexa Fluor 488 (1:200, AWS0005b, Abiowell) or CoraLite 594 (1:200, SA00013-4, Proteintech)- conjugated secondary antibodies for 2 h. Finally, samples were sealed with antifade mounting medium with DAPI (Beyotime, China) for fluorescence microscopy. Primary antibodies used included anti-p53 (1:200, 2524, Cell Signaling Technology) and anti-HMGB1 (1:250, ab79823, Abcam). Leica DM4 B Upright Microscope was used to take pictures.

Nuclear/cytoplasmic fractionation

Nuclear and cytoplasmic proteins were extracted using NE-PERTM Nuclear and Cytoplasmic Extraction Reagents (78833, Thermo Fisher) following the manufacturer's instructions. In brief, cells were first lysed in cytoplasmic extraction reagent I (CER I) containing proteinase inhibitor cocktail (NCM Biotech, China). Next, CER II was added to extract cytoplasmic contents. Nuclei were isolated by centrifugation, and the cytosolic fraction supernatant was collected. The intact nuclei were then lysed in nuclear extraction reagent (NER) containing proteinase inhibitor cocktail (NCM Biotech, China). Both nuclear and cytoplasmic lysates were then subjected to immunoblotting.

Transmission electron microscopic analysis

Cell samples were collected, fixed with commercially available electron microscope fixed solution (G1102, Servicebio) at 4°C, and subsequently embedded and sectioned. Images were acquired using a transmission electron microscope (Hitachi, Japan).

Bioinformatic analysis

The peripheral-blood gene expression dataset (GSE73809) was obtained from the Gene Expression Omnibus (GEO) database (https://www.ncbi.nlm.nih.gov/gds/). The dataset comprised 11 aGVHD patients and 13 non-aGVHD patients, all of whom underwent allo-HSCT. Transcriptome analysis was performed on peripheral blood CD4&CD8 T cells. The 'limma' [27] package in R software was utilized for quartile normalization of all gene expression values and identifying differentially expressed genes (DEGs) between aGVHD and non-GVHD patients. Gene set enrichment analysis (GSEA) [28] was conducted with the 'clusterProfiler' package [29] in R software. Pathway signatures were obtained from MSigDB of the Broad Institute (https://www.gsea-msigdb.org/gsea/index.jsp). The threshold for significantly enriched functional annotations in GSEA was set at an adjusted P-value < 0.05.

Clinical Science (2024) **138** 1287–1304
https://doi.org/10.1042/CS20241144

RNA sequencing

CD4+ T cells from healthy individuals were treated with or without IFN-γ for 48 h. RNA extraction, purification, reverse transcription, library construction, and sequencing were performed at Shanghai Majorbio Bio-pharm Biotechnology Co., Ltd. (Shanghai, China), following manufacturer's instructions (Illumina, San Diego, CA). To identify DEGs between the two groups, the expression level of each transcript was calculated using the transcripts per million reads (TPM) method. RSEM [30] was employed to quantify gene abundances. GSEA was performed to identify significantly enriched signaling pathways.

Statistical analysis

SPSS 26.0 software was used for data analysis. All tests were repeated at least thrice. Continuous variables with a normal distribution were presented as mean ± standard deviation (SD), while non-normal variables were reported as median (interquartile range). Independent samples Student's test compared means of two continuous normally distributed variables, and one-way analysis of variance (ANOVA) compared means of three or more continuous normally distributed variables. Tukey's test and Tamhane's T2 test for multiple comparisons was used to compare each column's mean with all other means in the case of equal and unequal variances, respectively. Mann–Whitney *U* test and Kruskal–Wallis test were used, respectively, to compare means of two and three or more groups of variables not normally distributed. Significance was set at $P<0.05$. Bioinformatic statistical analyses of the transcriptome were performed using R software (Version 4.1.1) and R studio (Version 2021.09.0).

Results

Increased IFN-γ in the plasma induces the activation and proliferation of CD4+ T cells

Early studies have demonstrated a correlation between elevated serum levels of IFN-γ and increased severity of GVHD following allo-HSCT [31]. To validate these observations, blood samples were collected from patients with aGVHD (n=13) and those without aGVHD (n=14). After removing an extremely high value from aGVHD patient, the plasma levels of IFN-γ were markedly elevated in the aGVHD group compared with the non-aGVHD group (Figure 1A). Additionally, the results of gene set enrichment analysis (GSEA) for transcriptome data from gene expression dataset (GSE73809) in GEO database revealed a significant activation of the IFN-γ response, allograft rejection and inflammatory response pathway in T cells from aGVHD patients compared with the non-aGVHD group (Figure 1B). To confirm the activation of IFN-γ signaling pathway, Western blotting was performed, and the results showed an increased phosphorylated STAT1 (p-STAT1) protein, the downstream of IFN-γ signaling pathway [32], in CD4+ T cells from aGVHD patients by our patient cohort (Supplementary Figure S1). Furthermore, GSEA of CD4+ T cells from healthy individuals in the IFN-γ treated group (n=3) and negative control group (n=3) by RNA sequencing demonstrated significant activation of oxidative phosphorylation, interferon gamma response, IFN- α response, allograft rejection, IL-6 JAK STAT3 signaling, and inflammatory response signaling pathways in IFN-γ treated cells (Figure 1C). These findings suggest that increased IFN-γ in the plasma plays a crucial role in regulating T-cell functions and contributes to aGVHD development.

CD69 and CD40L are transmembrane proteins primarily expressed by activated CD4+ T cells [33–35]. To investigate the impact of IFN-γ on T-cell activation, normal CD4+ T cells were stimulated with IFN-γ in the absence of anti-CD3/CD28 antibodies for the indicated time. As depicted in Figure 1D, CD69 and CD40L expression significantly increased in CD4+ T cells following 24 and 48 h of IFN-γ treatment, respectively. Furthermore, to elucidate the role of IFN-γ in cell proliferation, normal CD4+ T cells were stimulated with IL-2 in the presence or absence of IFN-γ. The group treated with IFN-γ plus IL-2 exhibited robust proliferation compared with the group stimulated with IL-2 alone (Figure 1E). While IFN-γ is widely acknowledged for its key role in mediating chronic inflammatory and autoimmune diseases, recent evidence suggests a dual role of IFN-γ in inflammation [36]. In certain mouse models, IFN-γ has been shown to induce CD4+ T-cell apoptosis [37,38], and high doses of IFN-γ exhibit cytotoxic effects [39]. Therefore, we further investigated the impact of IFN-γ on cell apoptosis. The percentages of Annexin V and PI double-positive cell population were used for statistical quantification. As shown in Figure 1F, the apoptosis cell populations gradually increased from 24 to 96 h in both control and IFN-γ treated group, indicating a spontaneously time-dependent apoptosis in CD4+ T cells. Notably, IFN-γ treatment not only did not accelerate cell apoptosis but also slightly reduced it at 96 h compared with the time-matched controls. Collectively, these findings suggest that IFN-γ directly promotes the activation and proliferation of CD4+ T cells instead of inducing apoptosis.

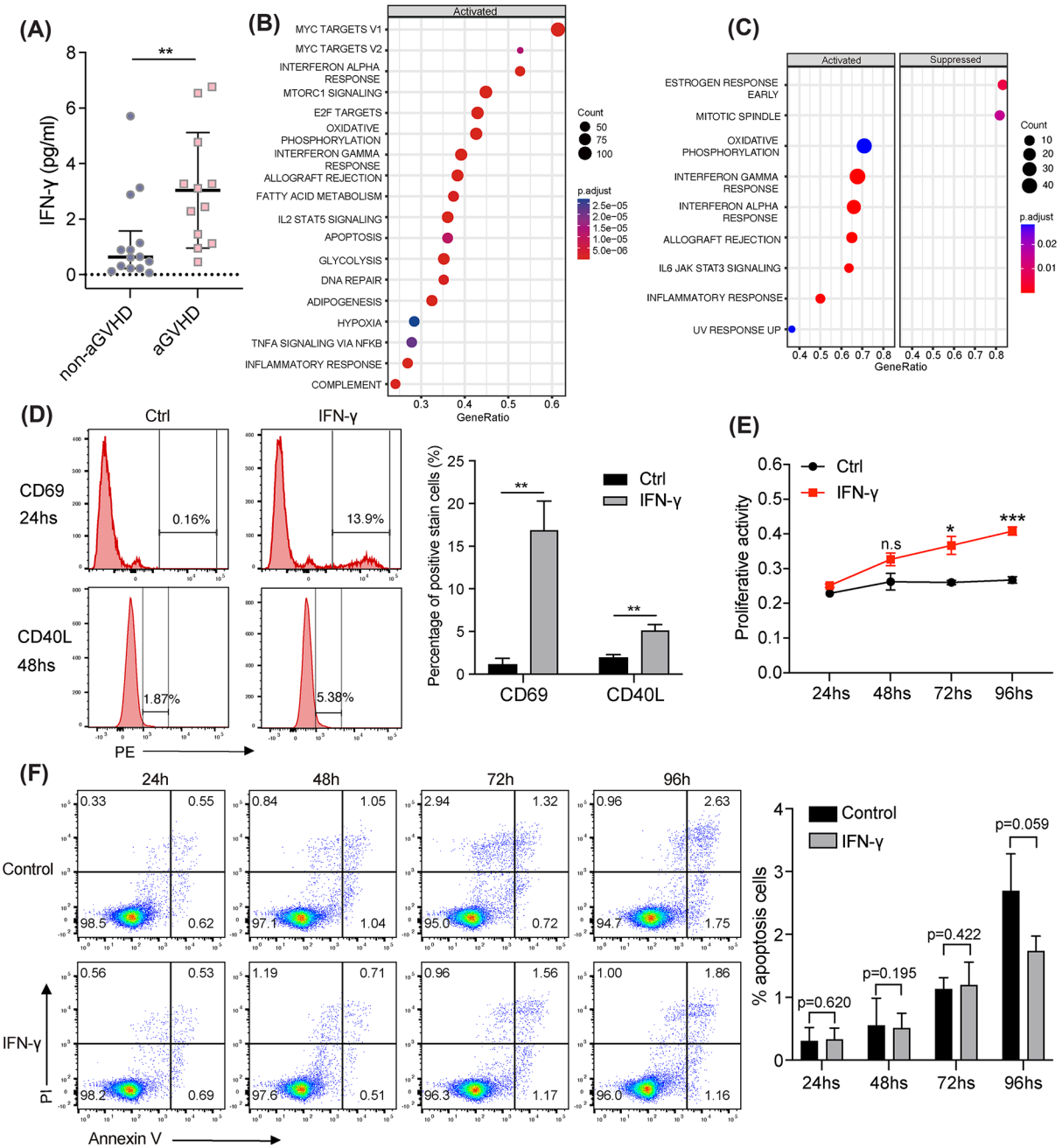

Figure 1. Impact of increased IFN-γ on CD4+ T cells

(**A**) Plasma IFN-γ levels in aGVHD patients (n=12) and the non-aGVHD group (n=14) were assessed by ELISA (Mann–Whitney U test). (**B**) GSEA of peripheral blood T cells between aGVHD and non-aGVHD patients (GSE73809 dataset). Pathway signatures source from hallmark gene sets. Count represents the number of 'core genes' which are high-expressed in activated pathways or low-expressed in suppressed pathways, having significant contribution to the pathway status. GeneRatio is the ratio of Count to the total number of genes in the pathways contained in the dataset. GSEA, gene set enrichment analysis. (**C**) GSEA of normal CD4+ T cells treated with IFN-γ (50 ng/ml) for 48 h and negative control group by RNA sequencing. Pathway signatures source from hallmark gene sets. (**D**) Flow cytometry analysis of CD69 and CD40L expression in normal CD4+ T cells treated with IFN-γ (50 ng/ml) for 24 and 48 h, respectively (unpaired Student's t-test). (**E**) Proliferation assessment of normal CD4+ T cells stimulated with or without IFN-γ (50 ng/ml) in the presence of IL-2 (100 IU/ml). Mann–Whitney U test was used to identify significant difference in 48 h group. P-values in 72 and 96 h group were determined by unpaired Student's test. (**F**) Flow cytometry analysis of apoptosis in normal CD4+ T cells treated with IFN-γ (50 ng/ml) for varying durations (unpaired Student's test). Data represent means ± SD from three independent experiments. n.s., not significant, *P<0.05, **P<0.01, ***P<0.001.

Clinical Science (2024) **138** 1287–1304
https://doi.org/10.1042/CS20241144

IFN-γ induces the autophagy-dependent degradation of p53 In CD4+ T cells

To determine the autophagy status of CD4+ T cells during aGVHD, CD4+ T cells from aGVHD patients and non-aGVHD group were subjected to transmission electron microscopy (TEM) to observe autophagosome-like structures. The results showed that CD4+ T cells from aGVHD patients exhibited an increased presence of autophagosomes compared with the non-aGVHD group (Figure 2A,B). Subsequently, cells were processed to obtain whole extracts. Western blotting results in Supplementary Figure S2 suggested that LC3-II/I ratio increased and p62/SQSTM1 expression decreased in CD4+ T cells from aGVHD patients relative to the non-aGVHD group. LC3 II/I and p62/SQSTM1 are autophagy biomarkers. In addition, we reanalyzed the transcriptome data from GSE73809 dataset. GSEA based on reactome annotation indicated that selective autophagy signaling pathway significantly enriched in aGVHD patients (Supplementary Figure S3). Taken together, these results suggest that the autophagic activity increased in CD4+ T cells from aGVHD patients. Furthermore, to investigate the potential of IFN-γ to induce autophagy in CD4+ T cells, we analyzed the LC3-II/I ratio and p62/SQSTM1 levels through Western blotting and observed ultrastructural changes using TEM in normal CD4+ T cells following IFN-γ stimulation to assess the autophagic process. It is well-known that IFN-γ induces genes transcription primarily though the JAK/STAT1 (Janus kinase/signal transducer and activator of transcription 1) signaling pathway [40]. JAK kinases phosphorylate intracellular STAT1 in response to extracellular IFN-γ signaling. Phosphorylated STAT1 (p-STAT1) then dimerize and translocate to the nuclear, binding to enhancers and promoters to regulate transcription of target genes [41]. Therefore, we measured the effect of IFN-γ by detecting p-STAT1 expression in the present study. Western blotting results demonstrated an increased LC3-II/I ratio and a corresponding degradation of p62/SQSTM1 protein in IFN-γ-treated cells (Figure 2C). Specifically, LC3-II/I ratio gradually increased after IFN-γ stimulation for 24 to 48 h and slightly reduced at 72 h, having significant difference at 48 and 72 h compared with control group. Meanwhile, p62/SQSTM1 expression gradually reduced following IFN-γ treatment, remarkably changing at both 48 and 72 h. These data preliminarily suggested that autophagic activity in CD4+ T cells significantly increased and reached its saturation at 48 h upon IFN-γ treatment. Consequently, 48 h was mainly used for subsequent research. Ultrastructural analysis revealed an augmentation in the formation of autophagosomes in CD4+ T cells upon IFN-γ treatment for 48 h (Figure 2D). These findings indicate that IFN-γ enhances autophagic activity in CD4+ T cells.

To explore whether IFN-γ influenced the expression of p53, normal CD4+ T cells were treated with IFN-γ for the designated time. Real-time PCR indicated no significant difference in p53 expression between IFN-γ-treated and untreated cells (Figure 2E). However, Western blotting illustrated a time-dependent reduction in p53 protein levels following IFN-γ treatment with a striking decrease starting from 48 h (Figure 2F). Intriguingly, as previously mentioned, autophagic activity in CD4+ T cells gradually increased and reached its saturation at 48 h after IFN-γ treatment. From this perspective, p53 degradation occurred later than the onset of autophagy, implying the possibility of autophagy-dependent degradation of p53 induced by IFN-γ. Considering proteasome system is tightly correlated with p53 degradation [42], we used proteasome inhibitor MG132 to inhibit proteasomal activity and then analyzed p53 protein levels under IFN-γ stimulation. Both MG132 (1 μM) and IFN-γ were added at the same time, treating cells for 24 h. In line with other study [43], our results showed that p53 expression was similar in MG132 treated CD4+ T cells to control cells, without long-term accumulation. Notably, IFN-γ decreased p53 expression when the proteasome pathway was inhibited, suggesting IFN-γ-mediated p53 degradation was independent of proteasome (Figure 2G). Furthermore, to ascertain whether IFN-γ-induced degradation of p53 is autophagy-dependent, normal CD4+ T cells were treated with IFN-γ for 48 h in the presence or absence of 3-methyladenine (3-MA) and chloroquine (CQ), inhibitors of autophagy and lysosome function, respectively. CD4+ T cells were pre-incubated with 3-MA (5 mM) or CQ (10 μM) for 2 h before IFN-γ treatment. Western blotting results demonstrated that the degradation of p53 induced by IFN-γ was efficiently prevented by both 3-MA (Figure 2H) and CQ (Figure 2I). These findings demonstrate that IFN-γ induces autophagy-dependent degradation of p53 in CD4+ T cells.

IFN-γ accelerates the autophagic degradation of p53 by inducing its nuclear export

Recent studies indicate that protein degradation by autophagy primarily occurs in the cytoplasm [7], while p53, functioning as a transcription factor, predominantly localizes in the nucleus. Therefore, we investigated whether IFN-γ induces the nuclear export of p53, leading to its degradation via autophagy in the cytoplasm of CD4+ T cells. Initially, we assessed the subcellular distribution of p53 in CD4+ T cells from both aGVHD and non-aGVHD patients. Immunocytochemistry staining results in Figure 3A revealed a significant reduction in nuclear p53 in CD4+ T cells from aGVHD patients compared with the non-aGVHD group. Western blotting analysis showed decreased nuclear

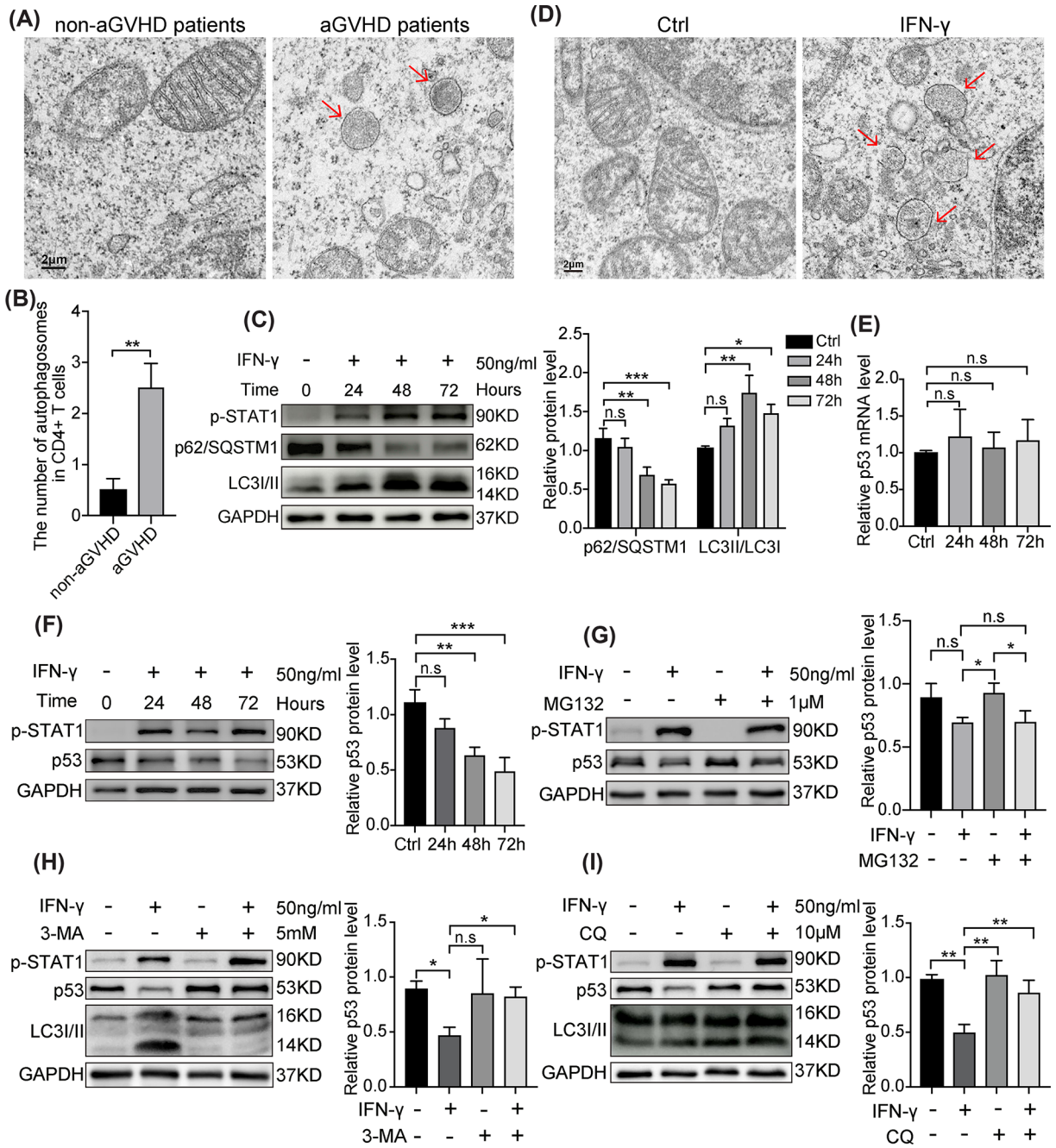

Figure 2. IFN-γ-mediated autophagy-dependent p53 degradation

(**A**) TEM of CD4+ T cells from aGVHD and non-aGVHD patients, showing autophagosome-like structures (indicated by red arrows). TEM, transmission electron microscopy. (**B**) The autophagosomes were quantified per TEM field from 10 randomly selected fields (Mann–Whitney *U* test). (**C**) Western blots depicting LC3 and p62/SQSTM1 expression in untreated and IFN-γ-treated normal CD4+ T cells (one-way ANOVA with Tukey's test). (**D**) TEM of normal CD4+ T cells treated with or without IFN-γ (50 ng/ml) for 48 h, highlighting autophagosome-like structures (indicated by red arrows). (**E**) Measurement of relative p53 mRNA levels in normal CD4+ T cells treated with 50 ng/ml IFN-γ over different durations (one-way ANOVA with Tukey's test). (**F**) Western blots illustrating p53 expression in untreated and IFN-γ-treated normal CD4+ T cells (one-way ANOVA with Tukey's test). (**G**) Western blots displaying the impact of proteasome inhibitor MG132 on IFN-γ-induced p53 degradation. Cells were treated with IFN-γ in the absence or presence of MG132 (1 μM) added at the same time as IFN-γ for 24 h (one-way ANOVA with Tukey's test). (**H–I**) Western blots showing the impact of autophagy pathway inhibitor on IFN-γ-induced p53 degradation using 3-MA (**H**) and CQ (**I**). Cells were treated with IFN-γ for 48 h in the absence or presence of 3-MA (5 mM) or CQ (10 μM) for 2 h before IFN-γ treatment. One-way ANOVA with Tamhane's T2 test (**H**) or Tukey's test (**I**) was used to identify significant differences. Scale bar: 2 μm. 3-MA, 3-methyladenine; CQ, chloroquine. Data represent mean ± SD from three independent experiments. n.s., not significant; **P*<0.05, ***P*<0.01, ****P*<0.001.

Clinical Science (2024) **138** 1287–1304
https://doi.org/10.1042/CS20241144

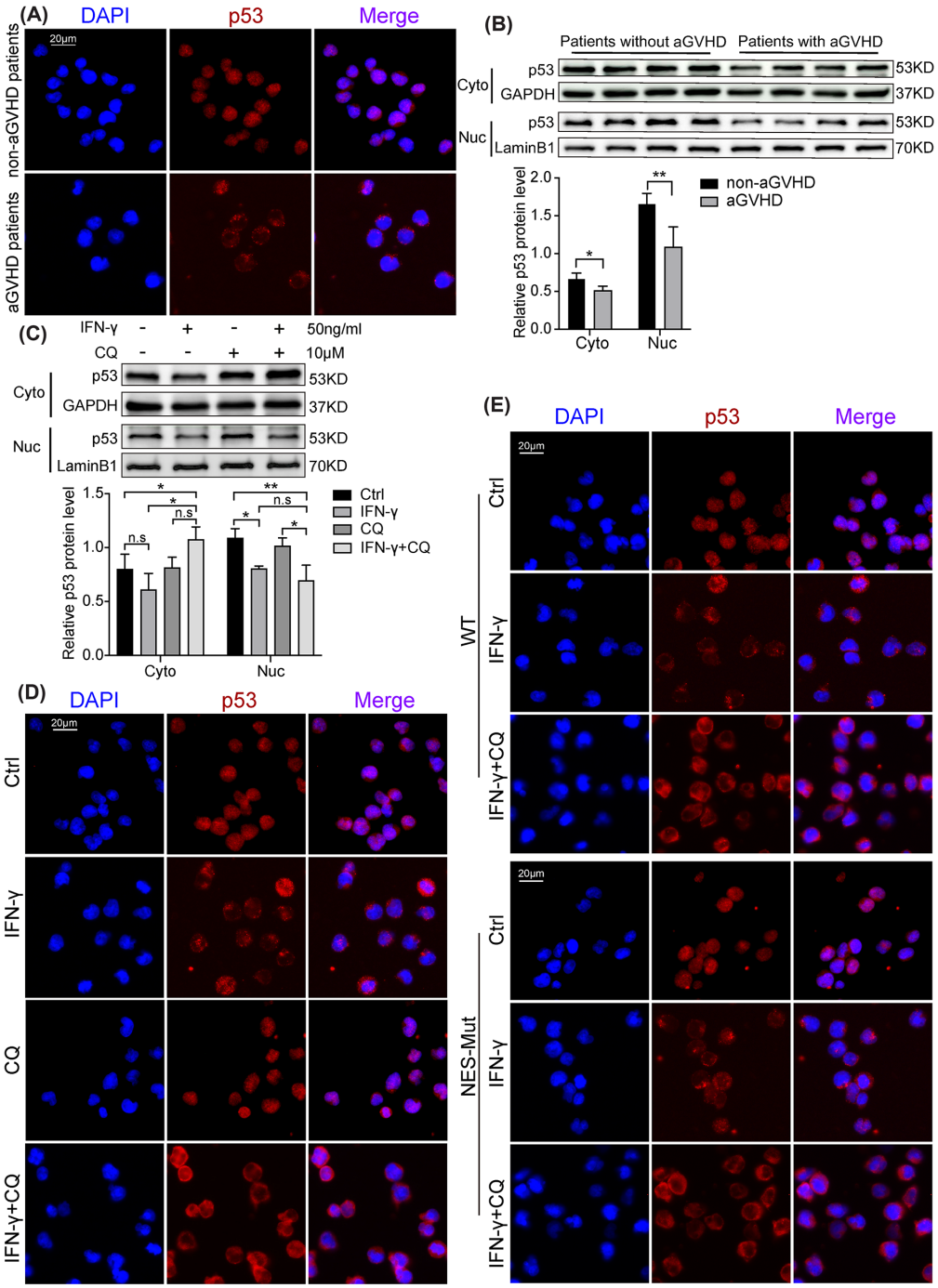

Figure 3. IFN-γ facilitates p53 autophagic degradation by inducing its nuclear export

(**A**) Immunocytochemistry for p53 and nuclear staining by DAPI in CD4+ T cells from aGVHD and non-aGVHD patients. (**B**) Western blots depicting cytoplasmic and nuclear p53 distribution in CD4+ T cells from aGVHD and non-aGVHD patients. The gray values of cytoplasmic p53 from eight patients were normalized to corresponding GAPDH respectively, so did the nuclear p53, which were normalized to Lamin B1. Then the relative gray values were used for statistical quantification (unpaired Student's *t*-test). (**C**) Western blots illustrating cytoplasmic and nuclear p53 distribution in normal CD4+ T cells treated with 50 ng/ml IFN-γ for 48 h in the absence or presence of 10 μM CQ added 2 h before IFN-γ addition (one-way ANOVA with Tukey's test). (**D**) Immunocytochemistry for p53 and nuclear staining by DAPI in normal CD4+ T cells treated similarly to (C). (**E**) Fluorescence microscope observed the RFP-tagged p53 protein in CD4+ T cells transfected with wild-type TP53 or mutant TP53 L348,350A plasmids. Cells treated with 50 ng/ml IFN-γ for 48 h in the absence or presence of 10 μM CQ added 2 h before IFN-γ addition. Scale bar: 20 μm. CQ, chloroquine; RFP, red fluorescent protein. Data represent means ± SD from three independent experiments. n.s., not significant; $^{*}P<0.05$, $^{**}P<0.01$.

and cytosolic fractions of p53 in CD4+ T cells from aGVHD patients relative to the non-aGVHD group, consistent with immunocytochemistry results (Figure 3B). Additionally, we employed immunocytochemistry staining and Western blotting to investigate the impact of IFN-γ on the subcellular localization of p53 in normal CD4+ T cells. The results indicated that p53 predominantly localised in the nuclear region of unstimulated (control) CD4+ T cells, while it decreased in the nucleus and cytoplasm after IFN-γ stimulation. Notably, treating cells with CQ alone resulted in a nuclear-dominant without reduction in both nuclear and cytoplasm distribution of p53. However, when cells were stimulated with IFN-γ in the presence of CQ, nuclear p53 significantly decreased compared with control and CQ alone treatment, while cytoplasmic p53 increased relative to control and the group stimulated with IFN-γ alone (Figure 3C,D). These results suggest the possibility that IFN-γ induces the nuclear export of p53, facilitating its autophagy-dependent degradation in the cytoplasm of CD4+ T cells.

Early work identified that p53 possesses three nuclear localization signals (NLSs) [44] together with two nuclear export signals (NESs) [45], which regulate its subcellular localization. To further explore the mechanism of IFN-γ-induced p53 nuclear-to-cytoplasm shift, we mutated the L348,350 of TP53 from L (lysine) to A (alanine) to acquire a NES-mutated TP53 (TP53 L348,350A mutant). The analogous mutations have been reported to efficiently prevent p53 nuclear export [45]. Then we constructed two types of pEX-6 (pGCMV/MCS/RFP/Neo) tagged plasmids expressing wild-type TP53 or mutant TP53 L348,350A, and transfected them into CD4+ T cells. Next, cells were exposed to IFN-γ for 48 h in the presence or absence of CQ. Fluorescence microscope was used to observe the red fluorescent protein (RFP) tagged p53 protein in transfected cells. Intriguingly, NES mutation had no impact on IFN-γ-induced nuclear-to-cytoplasm translocation and autophagic degradation of p53 (Figure 3E), implying that IFN-γ-mediated p53 nuclear export was independent on its NES, and other mechanism might involve in this process.

IFN-γ up-regulates HMGB1 expression and induces its nucleus-to-cytoplasm transport

To assess the impact of IFN-γ on HMGB1 expression, both mRNA and protein levels of HMGB1 were examined in normal CD4+ T cells following IFN-γ treatment. real-time PCR (Figure 4A) and western blotting (Figure 4B) results demonstrated a time-dependent up-regulation of HMGB1 expression by IFN-γ. Additionally, to elucidate the role of IFN-γ in HMGB1 subcellular localization, separate measurements of HMGB1 protein levels in the nucleus and cytosol were performed. The results revealed a decrease in the nuclear and an increase in the cytoplasm of HMGB1 in CD4+ T cells under IFN-γ stimulation (Figure 4C). Immunocytochemistry analysis results showed that HMGB1 mainly distributed in the nuclear of unstimulated (control) CD4+ T cells, while it decreased in the nuclear and increased in the cytoplasm after IFN-γ stimulation. Treating cells with CQ alone did not alter the localization of HMGB1. However, when stimulating cells with IFN-γ in the presence of CQ, HMGB1 staining exhibited as similar as IFN-γ alone stimulation (Figure 4D). Concurrently, observations in CD4+ T cells from aGVHD patients indicated reduced nuclear HMGB1 and increased cytoplasmic accumulation, as determined by immunocytochemistry and Western blotting analysis (Figure 4E,F). These findings collectively suggested that IFN-γ up-regulates HMGB1 expression, prompting its nuclear-to-cytoplasm translocation and cytoplasmic accumulation in CD4+ T cells.

HMGB1 is crucial for the nuclear export and autophagic degradation of p53 induced by IFN-γ

Previous studies have demonstrated the direct and dynamic interaction between HMGB1 and p53 in the nucleus and cytosol [24]. To investigate the impact of IFN-γ on the p53-HMGB1 interaction, immunoprecipitation was applied to analyze the interaction between these two proteins. Considering the autophagic degradation of p53 under IFN-γ stimulation, we pretreated cells with CQ (10 μM) for 2 h before IFN-γ addition. As shown in Figure 5A, IFN-γ strengthened the interaction between p53 and HMGB1 in the presence of CQ. To explore whether HMGB1 involved in the autophagic degradation of p53 induced by IFN-γ, HMGB1 was knocked down in normal CD4+ T cells (Figure 5B). Subsequent assessment of p53 expression upon IFN-γ stimulation demonstrated that HMGB1 deletion almost entirely prevented autophagic degradation of p53 (Figure 5C). Furthermore, the nucleus-to-cytoplasm transport of p53 initiated by IFN-γ was significantly inhibited in HMGB1$^{-/-}$ cells (Figure 5D). Conversely, IFN-γ directly induced HMGB1 transportation from the nucleus to cytoplasm in the absence of p53 (Figure 5E,F). These findings suggest that HMGB1 plays a pivotal role in IFN-γ-induced translocation of p53 from the nucleus to the cytoplasm and subsequent degradation via the autophagy pathway.

Clinical Science (2024) **138** 1287–1304
https://doi.org/10.1042/CS20241144

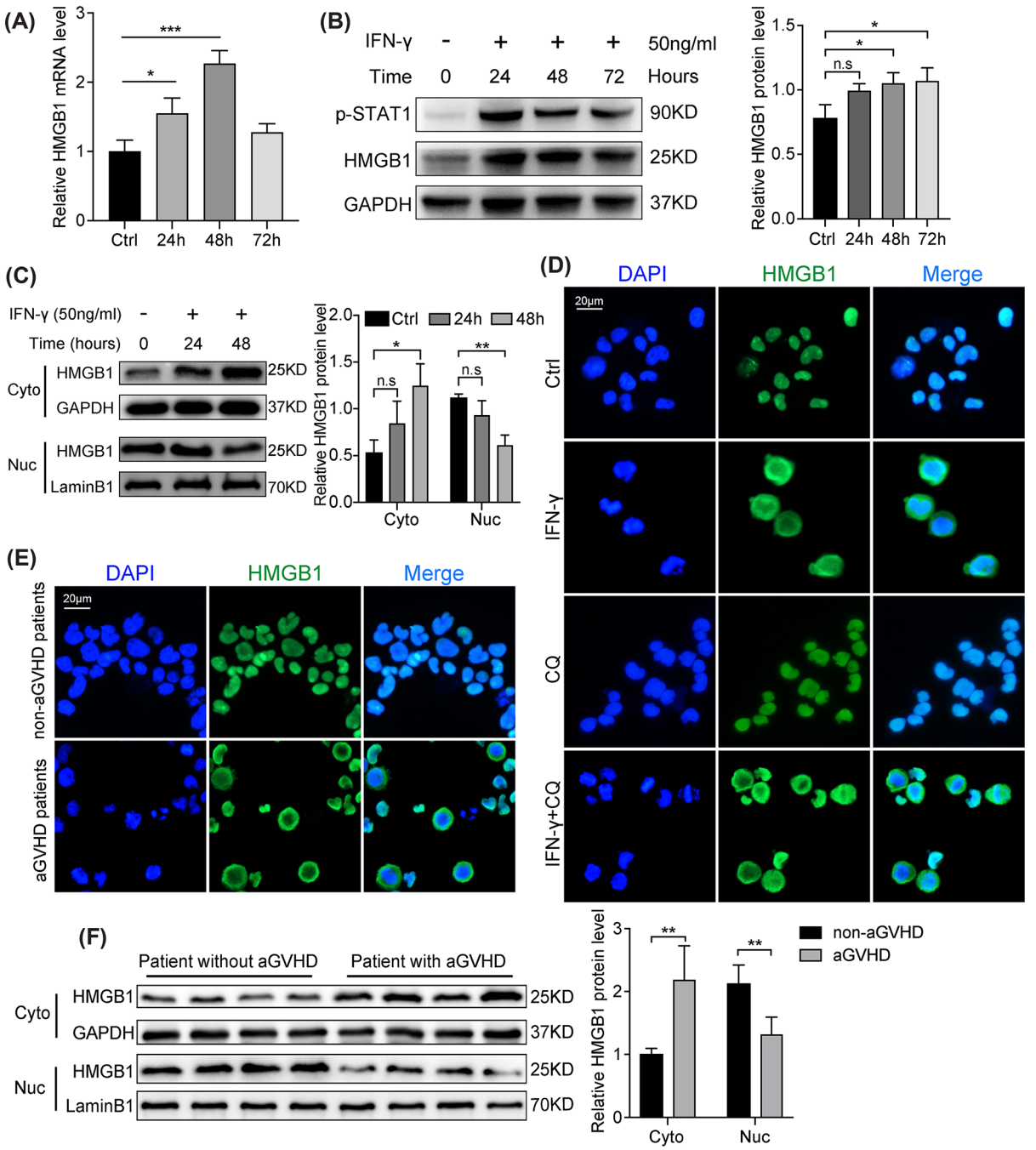

Figure 4. IFN-γ regulates HMGB1 expression and subcellular distribution

(**A**) Relative HMGB1 mRNA levels in normal CD4+ T cells treated with 50 ng/ml IFN-γ over different durations (one-way ANOVA with Tukey's test). (**B**) Western blots depicting HMGB1 expression in untreated and IFN-γ-treated normal CD4+ T cells (one-way ANOVA with Tukey's test). (**C**) Western blots showing cytoplasmic and nuclear HMGB1 distribution in normal CD4+ T cells treated with 50 ng/ml IFN-γ over different durations (one-way ANOVA with Tukey's test). (**D**) Immunocytochemistry for HMGB1 and nuclear staining by DAPI in normal CD4+ T cells treated with 50 ng/ml IFN-γ for 48 h in the absence or presence of 10 μM CQ added 2 h before IFN-γ addition. (**E**) Immunocytochemistry for HMGB1 and nuclear staining by DAPI in CD4+ T cells from aGVHD and non-aGVHD patients. (**F**) Western blots illustrating cytoplasmic and nuclear HMGB1 distribution in CD4+ T cells from aGVHD and non-aGVHD patients. The gray values of cytoplasmic HMGB1 from 8 patients were normalized to corresponding GAPDH respectively, so did the nuclear HMGB1, which were normalized to Lamin B1. Then the relative gray values were used for statistical quantification (unpaired Student's *t*-test). Scale bar: 20 μm. CQ, chloroquine. Data represent mean ± SD from three independent experiments. n.s., not significant; $^{*}P<0.05$, $^{**}P<0.01$, $^{***}P<0.001$.

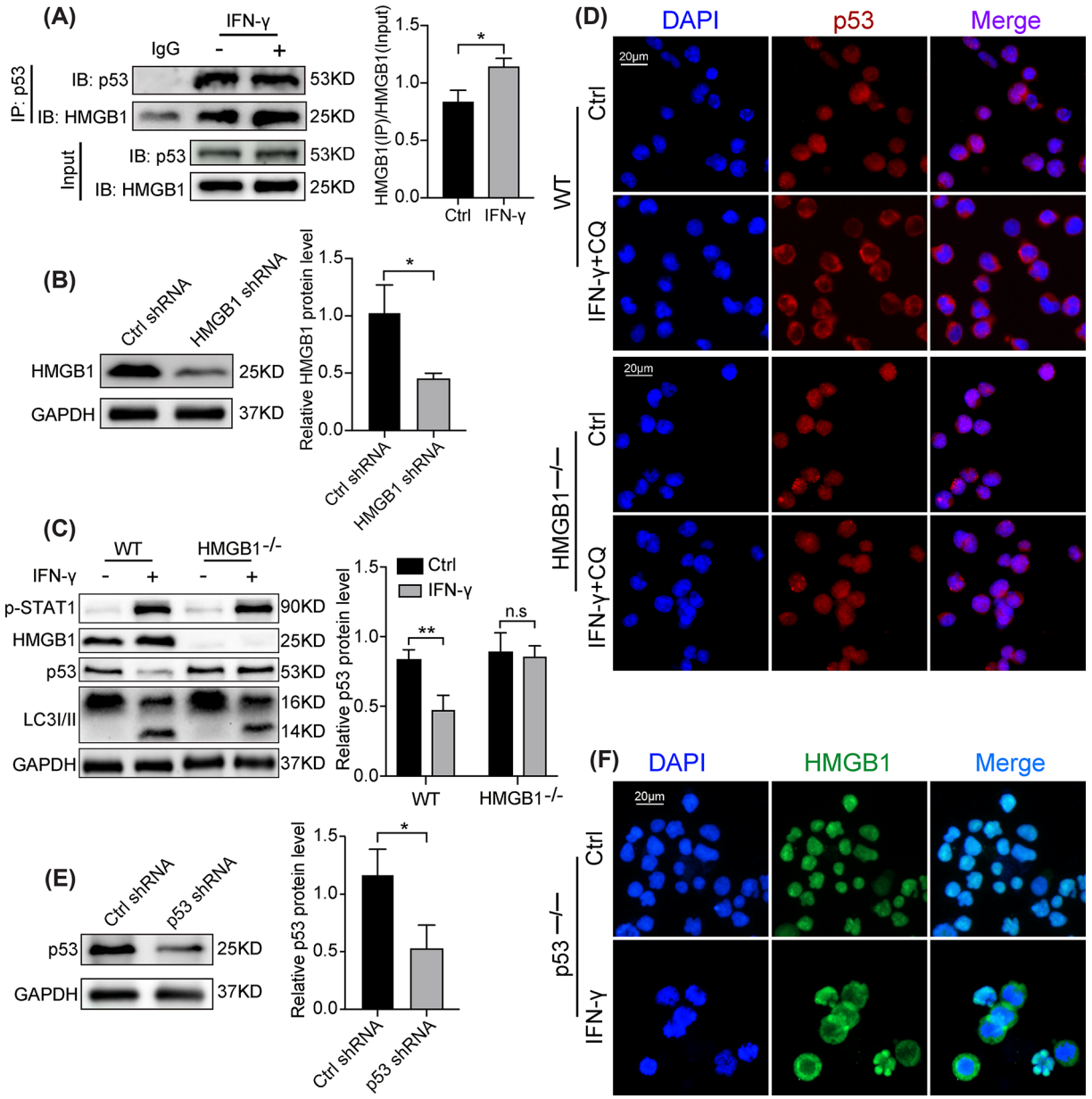

Figure 5. HMGB1 is crucial for IFN-γ-induced nuclear export and autophagic degradation of p53

(**A**) Co-immunoprecipitation with anti-p53 antibodies in untreated and IFN-γ-treated normal CD4+ T cells; Western blotting was performed to detect p53 and HMGB1 complex. Cells were treated with or without IFN-γ (50 ng/ml) for 48 h in the presence of 10 μM CQ added 2 h before the IFN-γ addition. The gray values of HMGB1 in each treatment group from immunoprecipitation samples were normalized to which from input samples respectively. *P*-values were determined using unpaired Student's *t*-test. (**B**) Western blots showing HMGB1 protein levels in normal CD4+ T cells transfected with HMGB1 interference (HMGB1 shRNA) or negative control (Ctrl shRNA) plasmid (unpaired Student's *t*-test). (**C**) Western blots depicting the impact of HMGB1 knockout on IFN-γ-induced p53 degradation. Normal CD4+ T cells transfected with HMGB1 interference or negative control plasmid were treated with 50 ng/ml IFN-γ for 48 h, respectively (unpaired Student's *t*-test). (**D**) Immunocytochemistry for p53 and nuclear staining in untreated or IFN-γ/CQ-treated wild-type or HMGB1$^{-/-}$ normal CD4+ T cells. Cells were treated with IFN-γ (50 ng/ml) for 48 h in the presence of 10 μM CQ added 2 h before the IFN-γ addition. (**E**) Western blots illustrating p53 protein levels in normal CD4+ T cells transfected with p53 interference (p53 shRNA) or negative control (Ctrl shRNA) plasmid (unpaired Student's *t*-test). (**F**) Immunocytochemistry for HMGB1 and nuclear staining in untreated or IFN-γ-treated p53$^{-/-}$ normal CD4+ T cells. Cells were treated with 50 ng/ml IFN-γ for 48 h. Scale bar: 20 μm. CQ, chloroquine. Data represent mean ± SD from three independent experiments. n.s., not significant; **P*<0.05, ***P*<0.01.

Clinical Science (2024) **138** 1287–1304
https://doi.org/10.1042/CS20241144

Discussion

Early investigations in GVHD models propose IFN-γ as a pathogenic factor in alloreactive responses. Genetic deletion of IFNGR in T cells averts lethal GVHD while preserving the robust GVT effect [46]. However, owing to the complexity and context-dependent nature of IFN signaling, it plays a pleiotropic role in GVHD effects. Some studies posit that IFN-γ might negatively regulate alloreactive T cells, thereby mitigating tissue damage [40,47,48]. Consistent with earlier finding [31], we detected an increase of plasma IFN-γ levels in aGVHD patients compared with the non-aGVHD group. Moreover, we revealed that IFN-γ response, allograft rejection and inflammatory response signaling pathways were activated in both peripheral T cells from aGVHD patients and IFN-γ-treated normal CD4+ T cells. Furthermore, our results demonstrated that IFN-γ directly induces the activation of CD4+ T cells independent of TCR signaling, promotes cell proliferation without inducing apoptosis. These findings underscore the vital proinflammatory role of IFN-γ in mediating aGVHD.

Others have suggested, that induced autophagy during the generation of human Th1/Tc1 cells correlates with *in vivo* human T-cell activation and increased allogeneic GVHD [49]. Consistently, we observed an increased presence of autophagosomes in CD4+ T cells from aGVHD patients compared with the non-aGVHD group. Besides, we revealed that IFN-γ augmented the autophagic activity in normal CD4+ T cells. Building upon prior and current study, we propose that elevated IFN-γ levels in plasma represent a crucial immune-related factor inducing autophagy in CD4+ T cells, and the enhanced autophagic activity induced by IFN-γ may be the potential mechanism for IFN-γ-mediated CD4+ T cells activation during aGVHD. The autophagy pathway may emerge as a promising therapeutic target in aGVHD treatment.

Additionally, we demonstrated that IFN-γ decreased p53 protein levels without altering its mRNA level in CD4+ T cells. Proteasome inhibitor fails to impede IFN-γ-induced p53 protein degradation, whereas autophagic inhibitors efficiently prevent this process. These data support our speculation that IFN-γ accelerates autophagy-dependent p53 degradation in CD4+ T cells. As mentioned earlier, our previous findings showed that the deficiency of p53 in CD4+ T cells leads to cell over-activation and proliferation under IL-2 stimulation [6]. In this study, we observed that IFN-γ and IL-2 treatment mediated a stronger proliferation of CD4+ T cells compared with IL-2 stimulation alone. It is most likely that the activation and p53 deficiency in CD4+ T cells provoked by IFN-γ enhances cell reaction to IL-2. These findings demonstrate that IFN-γ promotes aGVHD development by facilitating p53 autophagic degradation in CD4+ T cells, providing additional insights into our prior study and underscoring the significance of p53 in aGVHD development.

Recent studies suggested that type I and type II IFN promotes HMGB1 hyperacetylation within nuclear localization signal (NLS) sites and subsequent nuclear export [50]. In the present study, we revealed that HMGB1 primarily locates in the cytoplasm of CD4+ T cells from aGVHD patients and IFN-γ can induce HMGB1 nuclear-to-cytoplasm shift in CD4+ T cells, which is consistent with other study. In addition, based on previous finding of increased HMGB1 expression in CD4+ T cells from aGVHD patients [21], our present result suggested that IFN-γ is an important factor to up-regulate HMGB1 expression. From this point of view, IFN-γ regulates the expression and subcellular localization of HMGB1 during aGVHD, while future work is required to confirm whether IFN-γ mediates aGVHD development through this process. Notably, other have shown that cytoplasmic HMGB1 can induce autophagy through interactions with Beclin 1, an important autophagy-related protein [51], localizing it to autophagosomes [52]. Combined with prior discussion, IFN-γ-induced HMGB1 cytosolic accumulation may be the mechanism for IFN-γ elevating autophagic activity in CD4+ T cells, thereby promoting cell activation and aGVHD occurrence.

In parallel, previous findings have indicated that loss of p53 induces autophagy by increasing HMGB1 cytosolic translocation and enhancing HMGB1-Beclin 1 interactions [24]. In this study, we demonstrated that IFN-γ promoted p53 autophagic degradation by inducing its translocation to the cytosol, and HMGB1 played an essential role in p53 nuclear export and subsequent autophagic degradation. Collectively, we propose that under IFN-γ treatment, the increased autophagy level probably mediated by HMGB1 cytosolic translocation, and HMGB1-dependent p53 nuclear export are indispensable factors for p53 autophagic degradation. The reduction of p53, in turn, may further promote autophagy process by facilitating HMGB1 cytosolic translocation. From this perspective, our research is a complement and improvement of prior study, which focuses on aGVHD and puts forward a comparatively integrated mechanism for p53 autophagic degradation, further unveiling the intrinsic connection between HMGB1, p53 and autophagy.

Moreover, others western blotting results have revealed that in the absence of HMGB1, p53 translocation to the cytosol increases, while it still predominantly locates in the nuclear [24]. Consistently, our immunocytochemistry results show a nuclear-dominant distribution of p53 in HMGB1$^{-/-}$ CD4+ T cells. However, additional quantitative research is necessary to determine whether there is nuclear-to-cytoplasm shift of p53. Taken the present findings

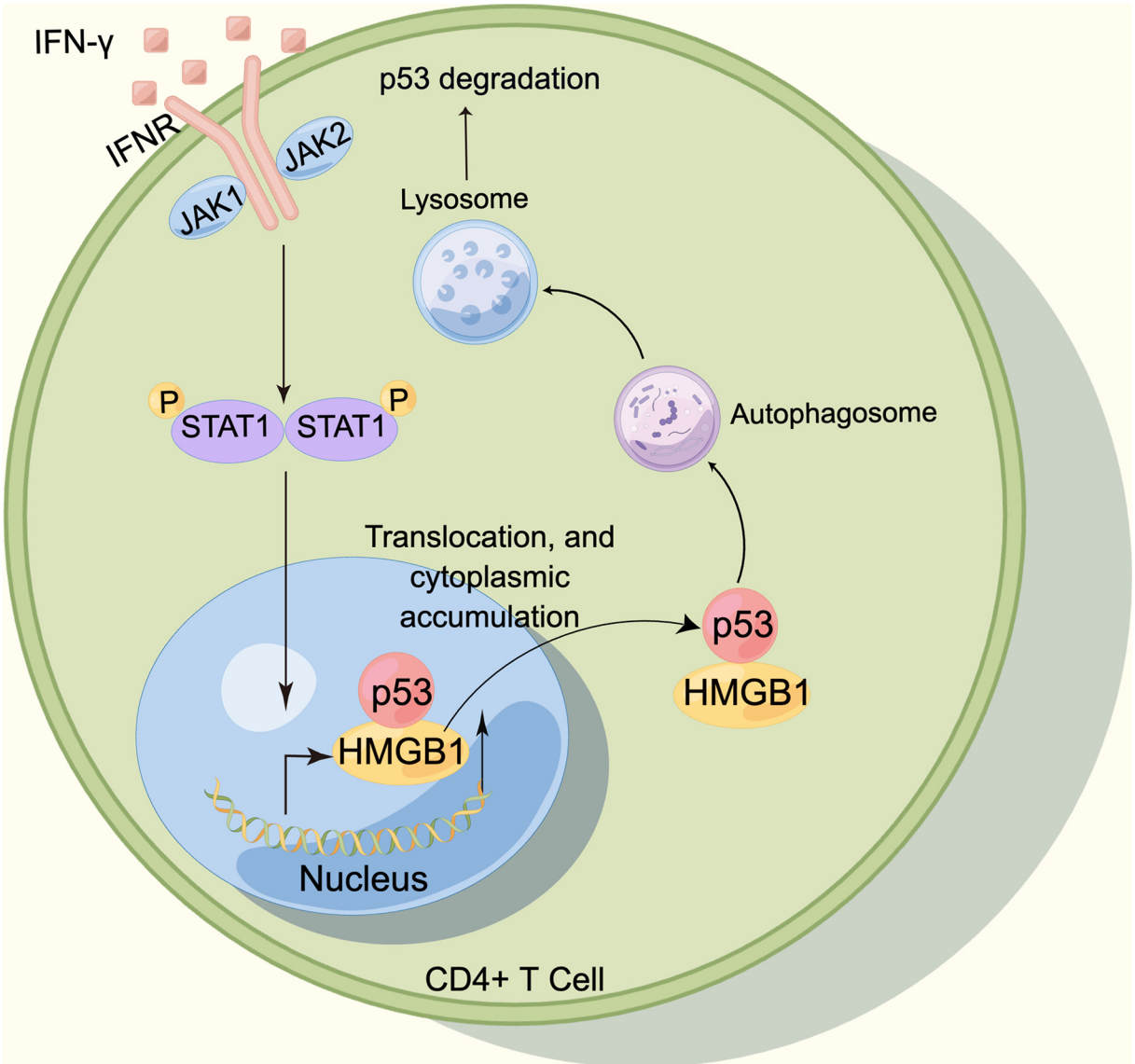

Figure 6. Schematic representation of IFN-γ-induced p53/HMGB1 complex nuclear-to-cytoplasm translocation and autophagic degradation of p53

Under aGVHD conditions, elevated plasma IFN-γ up-regulates HMGB1 mRNA and protein expression, enhancing the HMGB1-p53 interaction to form a complex in the nucleus. IFN-γ signaling induces HMGB1 translocation from the nucleus to the cytoplasm, transporting p53 to the cytoplasm, where it undergoes autophagy-dependent degradation.

together, we hypothesized that, under IFN-γ stimulation, the interaction between HMGB1 and p53 strengthened, forming a complex within the nucleus. IFN-γ-induced hyperacetylation of HMGB1 NLS sites emerged as a pivotal signal for its nuclear export. In this scenario, nuclear HMGB1 carried p53 transporting to the cytoplasm, where p53 subsequently underwent degradation through autophagy. The proposed model illustrating this process is depicted in Figure 6.

In conclusion, the present study provides evidence that IFN-γ promotes aGVHD development by facilitating HMGB1-mediated nuclear-to-cytoplasm translocation and autophagic degradation of p53 in CD4+ T cells. These findings advance our comprehension of the autophagy response in aGVHD, highlighting the correlation between aGVHD development and not only the total expression but also the subcellular localization of p53 and HMGB1. Importantly, this study unveils a novel pathway for p53 degradation, enhancing our understanding of the pivotal roles played by IFN-γ and p53 in the pathogenesis of aGVHD.

Clinical Science (2024) **138** 1287–1304
https://doi.org/10.1042/CS20241144

Clinical perspectives

- aGVHD poses a significant impediment to achieving a more favourable therapeutic outcome in allo-HSCT. Our prior investigations disclosed a correlation between p53 down-regulation in CD4+ T cells and the occurrence of aGVHD. However, the existence of additional mechanisms contributing to the reduction in p53 expression remains unclear.Point

- Our results demonstrated that heightened levels of IFN-γ in the plasma during aGVHD promote the activation, proliferation, and autophagic activity of CD4+ T cells. IFN-γ induced HMGB1-dependent nuclear-to-cytoplasm translocation and autophagic degradation of p53 in CD4+ T cells. HMGB1 underwent up-regulation and translocation from the nucleus to the cytoplasm following IFN-γ stimulation.

- These findings advance our comprehension of the autophagy response in CD4+ T cells during aGVHD, unveil a novel pathway for p53 degradation, and enhance our understanding of the pivotal roles played by IFN-γ and p53 in the pathogenesis of aGVHD.

Data Availability

All materials, data, and protocols are present in the manuscript or are available upon request. Publicly available dataset was analyzed in this study. These data can be found here: [https://www.ncbi.nlm.nih.gov/geo/query/acc.cgi?acc=gse73809].

Competing Interests

The authors declare that there are no competing interests associated with the manuscript.

Funding

This work was supported by the National Natural Science Foundation of China [grant number 81974002] and Translational Research Grant of NCRCH [grant number 2021WWC02].

CRediT Author Contribution

Shiyu Wang: Conceptualization, Data curation, Software, Supervision, Validation, Investigation, Visualization, Methodology, Writing—original draft, Project administration, Writing—review & editing. **Tingting Cheng:** Conceptualization, Data curation, Software, Validation, Investigation, Visualization, Methodology. **Xu Chen:** Conceptualization, Supervision, Methodology, Project administration. **Cong Zeng:** Conceptualization, Supervision, Methodology, Project administration. **Wei Qin:** Conceptualization, Supervision, Methodology. **Yajing Xu:** Conceptualization, Supervision, Funding acquisition, Methodology, Project administration, Writing—review & editing.

Ethics Approval

This study was approved by Human Ethics Committee of Xiangya School of Medicine, Central South University.

Abbreviations

aGVHD, acute graft-versus-host disease; 3-MA, 3-methyladenine; CER I, cytoplasmic extraction reagent I; CQ, chloroquine; DEG, differentially expressed gene; p-STAT1, phosphorylated STAT1; RFP, red fluorescent protein.

References

1 Korngold, R. and Sprent, J. (1978) Lethal graft-versus-host disease after bone marrow transplantation across minor histocompatibility barriers in mice. Prevention by removing mature T cells from marrow. *J. Exp. Med.* **148**, 1687–1698, https://doi.org/10.1084/jem.148.6.1687

2 Malard, F., Holler, E., Sandmaier, B.M., Huang, H. and Mohty, M. (2023) Acute graft-versus-host disease. *Nat. Rev. Dis. Primers* **9**, 27, https://doi.org/10.1038/s41572-023-00438-1

3 Kawashima, H., Takatori, H., Suzuki, K., Iwata, A., Yokota, M., Suto, A. et al. (2013) Tumor suppressor p53 inhibits systemic autoimmune diseases by inducing regulatory T cells. *J. Immunol.* **191**, 3614–3623, https://doi.org/10.4049/jimmunol.1300509

4 Leech, M., Xue, J.R., Dacumos, A., Hall, P., Santos, L., Yang, Y. et al. (2008) The tumour suppressor gene p53 modulates the severity of antigen-induced arthritis and the systemic immune response. *Clin. Exp. Immunol.* **152**, 345–353, https://doi.org/10.1111/j.1365-2249.2008.03629.x

5 Zheng, S.J., Lamhamedi-Cherradi, S.E., Wang, P., Xu, L. and Chen, Y.H. (2005) Tumor suppressor p53 inhibits autoimmune inflammation and macrophage function. *Diabetes* **54**, 1423–1428, https://doi.org/10.2337/diabetes.54.5.1423
6 Hua, J., Chen, Y., Fu, B., Chen, X., Xu, X.-J., Yang, S.-H. et al. (2020) Downregulation of p53 by insufficient CTCF in CD4 T cells is an important factor inducing acute graft-versus-host disease. *Front. Immunol.* **11**, 568637, https://doi.org/10.3389/fimmu.2020.568637
7 Mizushima, N., Yoshimori, T. and Levine, B. (2010) Methods in mammalian autophagy research. *Cell* **140**, 313–326, https://doi.org/10.1016/j.cell.2010.01.028
8 Behrends, C., Sowa, M.E., Gygi, S.P. and Harper, J.W. (2010) Network organization of the human autophagy system. *Nature* **466**, 68–76, https://doi.org/10.1038/nature09204
9 Li, C., Capan, E., Zhao, Y., Zhao, J., Stolz, D., Watkins, S.C. et al. (2006) Autophagy is induced in CD4+ T cells and important for the growth factor-withdrawal cell death. *J. Immunol.* **177**, 5163–5168, https://doi.org/10.4049/jimmunol.177.8.5163
10 Ge, Y., Huang, M. and Yao, Y.M. (2018) Autophagy and proinflammatory cytokines: Interactions and clinical implications. *Cytokine Growth Factor Rev.* **43**, 38–46, https://doi.org/10.1016/j.cytogfr.2018.07.001
11 Hubbard, V.M., Valdor, R., Patel, B., Singh, R., Cuervo, A.M. and Macian, F. (2010) Macroautophagy regulates energy metabolism during effector T cell activation. *J. Immunol.* **185**, 7349–7357, https://doi.org/10.4049/jimmunol.1000576
12 Robb, R.J. and Hill, G.R. (2012) The interferon-dependent orchestration of innate and adaptive immunity after transplantation. *Blood* **119**, 5351–5358, https://doi.org/10.1182/blood-2012-02-368076
13 Parampalli Yajnanarayana, S., Stübig, T., Cornez, I., Alchalby, H., Schönberg, K., Rudolph, J. et al. (2015) JAK1/2 inhibition impairs T cell function in vitro and in patients with myeloproliferative neoplasms. *Br. J. Haematol.* **169**, 824–833, https://doi.org/10.1111/bjh.13373
14 Gutierrez, M.G., Master, S.S., Singh, S.B., Taylor, G.A., Colombo, M.I. and Deretic, V. (2004) Autophagy is a defense mechanism inhibiting BCG and Mycobacterium tuberculosis survival in infected macrophages. *Cell* **119**, 753–766, https://doi.org/10.1016/j.cell.2004.11.038
15 Feng, C.G., Zheng, L., Lenardo, M.J. and Sher, A. (2009) Interferon-inducible immunity-related GTPase Irgm1 regulates IFN gamma-dependent host defense, lymphocyte survival and autophagy. *Autophagy* **5**, 232–234, https://doi.org/10.4161/auto.5.2.7445
16 Yang, S.L., Tan, H.X., Niu, T.T., Liu, Y.K., Gu, C.J., Li, D.J. et al. (2021) The IFN-γ-IDO1-kynureine pathway-induced autophagy in cervical cancer cell promotes phagocytosis of macrophage. *Int. J. Biol. Sci.* **17**, 339–352, https://doi.org/10.7150/ijbs.51241
17 He, Z., Yang, Y., Xing, Z., Zuo, Z., Wang, R., Gu, H. et al. (2020) Intraperitoneal injection of IFN-γ restores microglial autophagy, promotes amyloid-β clearance and improves cognition in APP/PS1 mice. *Cell Death Dis.* **11**, 440, https://doi.org/10.1038/s41419-020-2644-4
18 Javaherian, K., Liu, J.F. and Wang, J.C. (1978) Nonhistone proteins HMG1 and HMG2 change the DNA helical structure. *Science* **199**, 1345–1346, https://doi.org/10.1126/science.628842
19 Bustin, M. and Neihart, N.K. (1979) Antibodies against chromosomal HMG proteins stain the cytoplasm of mammalian cells. *Cell* **16**, 181–189, https://doi.org/10.1016/0092-8674(79)90199-5
20 Andersson, U. and Tracey, K.J. (2011) HMGB1 is a therapeutic target for sterile inflammation and infection. *Annu. Rev. Immunol.* **29**, 139–162, https://doi.org/10.1146/annurev-immunol-030409-101323
21 Xu, Y.J., Li, L., Chen, Y., Fu, B., Wu, D.S., Li, X.L. et al. (2015) Role of HMGB1 in regulation of STAT3 expression in CD4(+) T cells from patients with aGVHD after allogeneic hematopoietic stem cell transplantation. *Clin. Immunol.* **161**, 278–283, https://doi.org/10.1016/j.clim.2015.08.012
22 Rendon-Mitchell, B., Ochani, M., Li, J., Han, J., Wang, H., Yang, H. et al. (2003) IFN-gamma induces high mobility group box 1 protein release partly through a TNF-dependent mechanism. *J. Immunol.* **170**, 3890–3897, https://doi.org/10.4049/jimmunol.170.7.3890
23 Hao, J., Zhang, Y.J., Lv, X., Xu, N., Liu, Q.J., Zhao, S. et al. (2013) IFN-γ induces lipogenesis in mouse mesangial cells via the JAK2/STAT1 pathway. *Am. J. Physiol. Cell Physiol.* **304**, C760–C767, https://doi.org/10.1152/ajpcell.00352.2012
24 Livesey, K.M., Kang, R., Vernon, P., Buchser, W., Loughran, P., Watkins, S.C. et al. (2012) p53/HMGB1 complexes regulate autophagy and apoptosis. *Cancer Res.* **72**, 1996–2005, https://doi.org/10.1158/0008-5472.CAN-11-2291
25 Schoemans, H.M., Lee, S.J., Ferrara, J.L., Wolff, D., Levine, J.E., Schultz, K.R. et al. (2018) EBMT-NIH-CIBMTR task force position statement on standardized terminology & guidance for graft-versus-host disease assessment. *Bone Marrow Transplant.* **53**, 1401–1415, https://doi.org/10.1038/s41409-018-0204-7
26 Huang, Z., Zhong, Z., Zhang, L., Wang, X., Xu, R., Zhu, L. et al. (2015) Down-regulation of HMGB1 expression by shRNA constructs inhibits the bioactivity of urothelial carcinoma cell lines via the NF-κB pathway. *Sci. Rep.* **5**, 12807, https://doi.org/10.1038/srep12807
27 Ritchie, M.E., Phipson, B., Wu, D., Hu, Y., Law, C.W., Shi, W. et al. (2015) limma powers differential expression analyses for RNA-sequencing and microarray studies. *Nucleic. Acids. Res.* **43**, e47, https://doi.org/10.1093/nar/gkv007
28 Subramanian, A., Tamayo, P., Mootha, V.K., Mukherjee, S., Ebert, B.L., Gillette, M.A. et al. (2005) Gene set enrichment analysis: a knowledge-based approach for interpreting genome-wide expression profiles. *Proc. Natl. Acad. Sci. U.S.A.* **102**, 15545–15550, https://doi.org/10.1073/pnas.0506580102
29 Yu, G., Wang, L.G., Han, Y. and He, Q.Y. (2012) clusterProfiler: an R package for comparing biological themes among gene clusters. *OMICS* **16**, 284–287, https://doi.org/10.1089/omi.2011.0118
30 Li, B. and Dewey, C.N. (2011) RSEM: accurate transcript quantification from RNA-Seq data with or without a reference genome. *BMC Bioinformatics* **12**, 323, https://doi.org/10.1186/1471-2105-12-323
31 Imamura, M., Hashino, S., Kobayashi, H., Kubayashi, S., Hirano, S., Minagawa, T. et al. (1994) Serum cytokine levels in bone marrow transplantation: synergistic interaction of interleukin-6, interferon-gamma, and tumor necrosis factor-alpha in graft-versus-host disease. *Bone Marrow Transplant.* **13**, 745–751
32 Abboud, R., Choi, J., Ruminski, P., Schroeder, M.A., Kim, S., Abboud, C.N. et al. (2020) Insights into the role of the JAK/STAT signaling pathway in graft-versus-host disease. *Ther. Adv. Hematol.* **11**, 2040620720914489, https://doi.org/10.1177/2040620720914489

33 Danese, S., Sans, M. and Fiocchi, C. (2004) The CD40/CD40L costimulatory pathway in inflammatory bowel disease. *Gut* **53**, 1035–1043, https://doi.org/10.1136/gut.2003.026278
34 Noelle, R.J., Roy, M., Shepherd, D.M., Stamenkovic, I., Ledbetter, J.A. and Aruffo, A. (1992) A 39-kDa protein on activated helper T cells binds CD40 and transduces the signal for cognate activation of B cells. *Proc. Natl. Acad. Sci. U.S.A.* **89**, 6550–6554, https://doi.org/10.1073/pnas.89.14.6550
35 Yang, L., Xu, L.Z., Liu, Z.Q., Yang, G., Geng, X.R., Mo, L.H. et al. (2016) Interleukin-13 interferes with activation-induced t-cell apoptosis by repressing p53 expression. *Cell Mol. Immunol.* **13**, 669–677, https://doi.org/10.1038/cmi.2015.50
36 Mühl, H. and Pfeilschifter, J. (2003) Anti-inflammatory properties of pro-inflammatory interferon-gamma. *Int. Immunopharmacol.* **3**, 1247–1255, https://doi.org/10.1016/S1567-5769(03)00131-0
37 Dalton, D.K., Haynes, L., Chu, C.Q., Swain, S.L. and Wittmer, S. (2000) Interferon gamma eliminates responding CD4 T cells during mycobacterial infection by inducing apoptosis of activated CD4 T cells. *J. Exp. Med.* **192**, 117–122, https://doi.org/10.1084/jem.192.1.117
38 Liesenfeld, O., Kosek, J.C. and Suzuki, Y. (1997) Gamma interferon induces Fas-dependent apoptosis of Peyer's patch T cells in mice following peroral infection with Toxoplasma gondii. *Infect. Immun.* **65**, 4682–4689, https://doi.org/10.1128/iai.65.11.4682-4689.1997
39 Wu, J., Raman, A., Coffey, N.J., Sheng, X., Wahba, J., Seasock, M.J. et al. (2021) The key role of NLRP3 and STING in APOL1-associated podocytopathy. *J. Clin. Invest.* **131**, https://doi.org/10.1172/JCI136329
40 Wang, H. and Yang, Y.G. (2014) The complex and central role of interferon-γ in graft-versus-host disease and graft-versus-tumor activity. *Immunol. Rev.* **258**, 30–44, https://doi.org/10.1111/imr.12151
41 Aaronson, D.S. and Horvath, C.M. (2002) A road map for those who don't know JAK-STAT. *Science* **296**, 1653–1655, https://doi.org/10.1126/science.1071545
42 Esser, C., Scheffner, M. and Höhfeld, J. (2005) The chaperone-associated ubiquitin ligase CHIP is able to target p53 for proteasomal degradation. *J. Biol. Chem.* **280**, 27443–27448, https://doi.org/10.1074/jbc.M501574200
43 MacLaren, A.P., Chapman, R.S., Wyllie, A.H. and Watson, C.J. (2001) p53-dependent apoptosis induced by proteasome inhibition in mammary epithelial cells. *Cell Death Differ.* **8**, 210–218, https://doi.org/10.1038/sj.cdd.4400801
44 Shaulsky, G., Goldfinger, N., Ben-Ze'ev, A. and Rotter, V. (1990) Nuclear accumulation of p53 protein is mediated by several nuclear localization signals and plays a role in tumorigenesis. *Mol. Cell. Biol.* **10**, 6565–6577
45 Stommel, J.M., Marchenko, N.D., Jimenez, G.S., Moll, U.M., Hope, T.J. and Wahl, G.M. (1999) A leucine-rich nuclear export signal in the p53 tetramerization domain: regulation of subcellular localization and p53 activity by NES masking. *EMBO J.* **18**, 1660–1672, https://doi.org/10.1093/emboj/18.6.1660
46 Choi, J., Ziga, E.D., Ritchey, J., Collins, L., Prior, J.L., Cooper, M.L. et al. (2012) IFNγR signaling mediates alloreactive T-cell trafficking and GVHD. *Blood* **120**, 4093–4103, https://doi.org/10.1182/blood-2012-01-403196
47 Sun, K., Hsiao, H.H., Li, M., Ames, E., Bouchlaka, M., Welniak, L.A. et al. (2012) IFN-γ receptor-deficient donor T cells mediate protection from graft-versus-host disease and preserve graft-versus-tumor responses after allogeneic bone marrow transplantation. *J. Immunol.* **189**, 2033–2042, https://doi.org/10.4049/jimmunol.1102853
48 Welniak, L.A., Blazar, B.R., Anver, M.R., Wiltrout, R.H. and Murphy, W.J. (2000) Opposing roles of interferon-gamma on CD4+ T cell-mediated graft-versus-host disease: effects of conditioning. *Biol. Blood Marrow Transplant.* **6**, 604–612, https://doi.org/10.1016/S1083-8791(00)70025-5
49 Amarnath, S., Flomerfelt, F.A., Costanzo, C.M., Foley, J.E., Mariotti, J., Konecki, D.M. et al. (2010) Rapamycin generates anti-apoptotic human Th1/Tc1 cells via autophagy for induction of xenogeneic GVHD. *Autophagy* **6**, 523–541, https://doi.org/10.4161/auto.6.4.11811
50 Lu, B., Antoine, D.J., Kwan, K., Lundbäck, P., Wähämaa, H., Schierbeck, H. et al. (2014) JAK/STAT1 signaling promotes HMGB1 hyperacetylation and nuclear translocation. *Proc. Natl. Acad. Sci. U.S.A.* **111**, 3068–3073, https://doi.org/10.1073/pnas.1316925111
51 Kang, R., Zeh, H.J., Lotze, M.T. and Tang, D. (2011) The Beclin 1 network regulates autophagy and apoptosis. *Cell Death Differ.* **18**, 571–580, https://doi.org/10.1038/cdd.2010.191
52 Tang, D., Kang, R., Livesey, K.M., Cheh, C.W., Farkas, A., Loughran, P. et al. (2010) Endogenous HMGB1 regulates autophagy. *J. Cell Biol.* **190**, 881–892, https://doi.org/10.1083/jcb.200911078